Electronic Supplementary Material (ESI) for Dalton Transactions.

Regioselectivity in C–H Activation: reagent control in cyclometallation of 2-(1-naphthyl)-pyridine

Mikhail Kondrashov, David Provost and Ola F. Wendt*

Centre for Analysis and Synthesis, Department of Chemistry, Lund University, P. O. Box 124, S-221 00 Lund, Sweden. E-mail: ola.wendt@chem.lu.se

Contents

Crystallography

Table S1. Crystal data and refinement details for compounds **4** and **6**.

	4	**6**
Formula	$C_{25}H_{24}ClNRu$	$C_{15}H_{10}BF_2N$
Fw	474.97	253.05
Space group	$P2_1/n$	$P2_1/c$
Crystal system	monoclinic	monoclinic
T/K	293	293
a□/Å	7.9093(4)	7.9355(5)
b/Å	16.4319(8)	19.5025(11)
c/Å	16.0856(10)	8.0301(5)
β/deg	103.852(6)	111.383(7)
V/Å³	2029.8(2)	1157.21(13)
Z	4	4
D_{calcd} /g cm^{-3}	1.554	1.452
μ /mm^{-1}	0.914	0.106
θ-range /deg	2.48-28.93	2.76-30.03
No. reflns collected	14971	16901
No. of unique reflns	4668	3388
$R(F)$ $(I > 2\sigma(I))$[a]	0.0435	0.0495
$wR^2(F^2)$ (all data)[b]	0.1140	0.1392
S[c]	1.072	1.048
R_{int}	0.0592	0.0210
CCDC	1404269	1404270

[a] $R = \Sigma(|F_o| - |F_c|)/\Sigma|F_o|$. [b] $wR2 = [\Sigma w(F_o^2 - F_c^2)^2/\Sigma(F_o^2)^2]^{1/2}$.

[c] $S = [\Sigma w F_o^2 - F_c^2)^2/(n-p)]^{1/2}$.

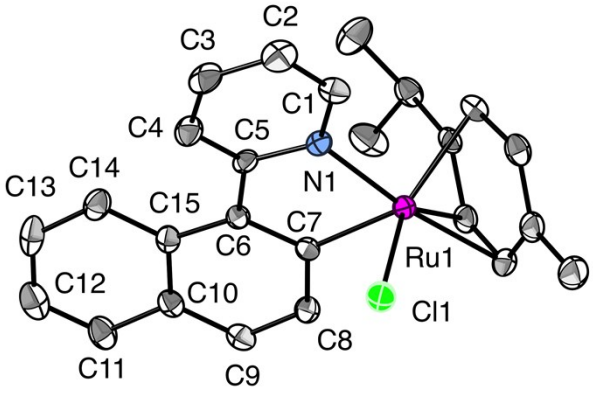

Figure S1. Molecular structure of **4** at the 30% probability level.

Table S2. Selected distances (Å) and angles (deg) in **4**:

Ru…N	2.088(3)	C(7)-Ru-C(21)	91.4(1)	N-C(5)-C(6)-C(7)	-10.2
Ru…C(7)	2.051(3)	C(7)-Ru-Cl	86.2(1)	N-Ru-C(16)-C(22)	41.0
Ru…Cl	2.4367(10)	N-Ru-Cl	85.2(1)	C(7)-C(6)-C(15)-C(14)	171.1
C(7)-Ru-N	76.6(1)	C(5)-C(6)-C(14)-H(14)	-14.3	C(25)-C(19)-Ru-Cl(1)	5.8
		C(5)-C(6)-C(7)-Ru	6.2	C(5)-C(6)-C(14)-H(14)	14.3

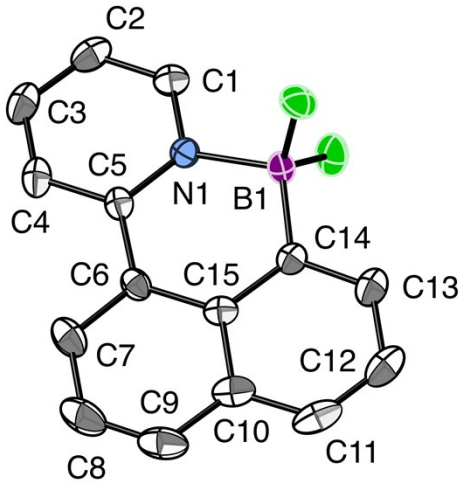

Figure S2. Molecular structure of **6** at the 30% probability level.

Table S3. Selected distances (Å) and angles (deg) in **6**:

B…N	1.604(2)	F(2)-B-F(1)	108.4(1)	C(15)-C(14)-B-N	-8.8
B…C(14)	1.576(2)	F(1)-B-N	106.5(1)	B-C(14)-C(6)-C(5)	4.7
B…F(2)	1.398(2)	N-B-C(14)	110.3(1)	C(6)-C(5) -N-B	8.2
B…F(1)	1.404(2)	C(15)-C(14)-B	121.6(1)	C(5)-N-B-C(14)	12.3

NMR Spectra

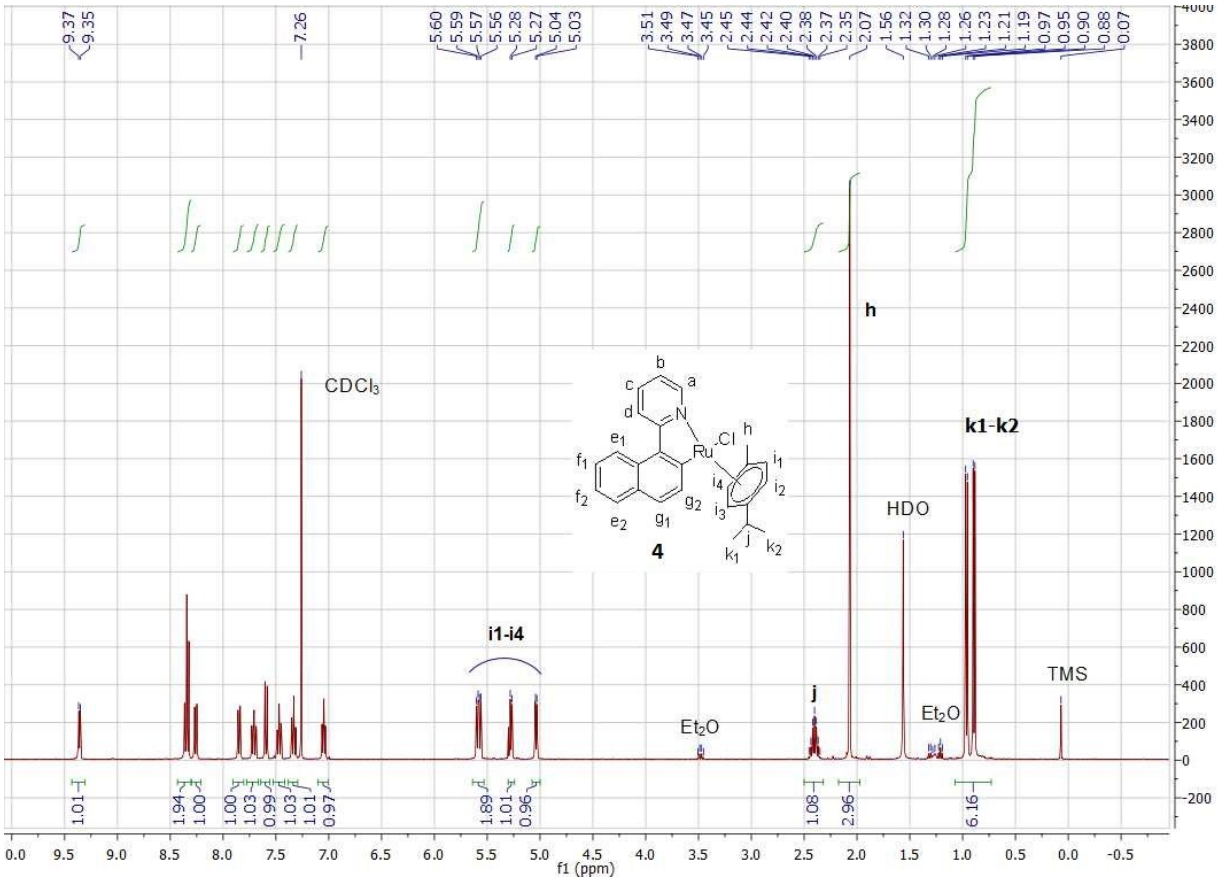

Figure S3. ^{1}H NMR spectrum (400 MHz, $CDCl_3$) of compound **4**

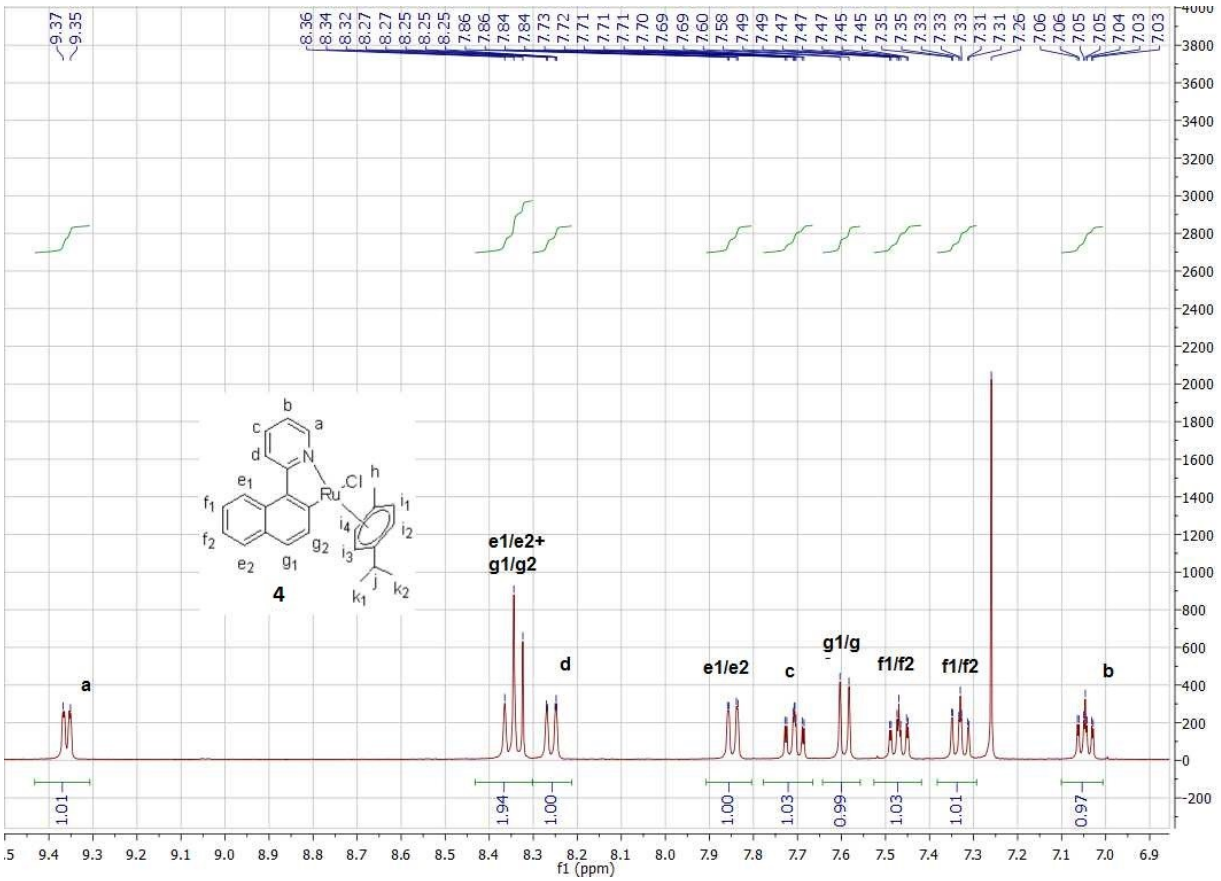

Figure S4. Aromatic region of the ^{1}H NMR spectrum (400 MHz, $CDCl_3$) of compound **4**

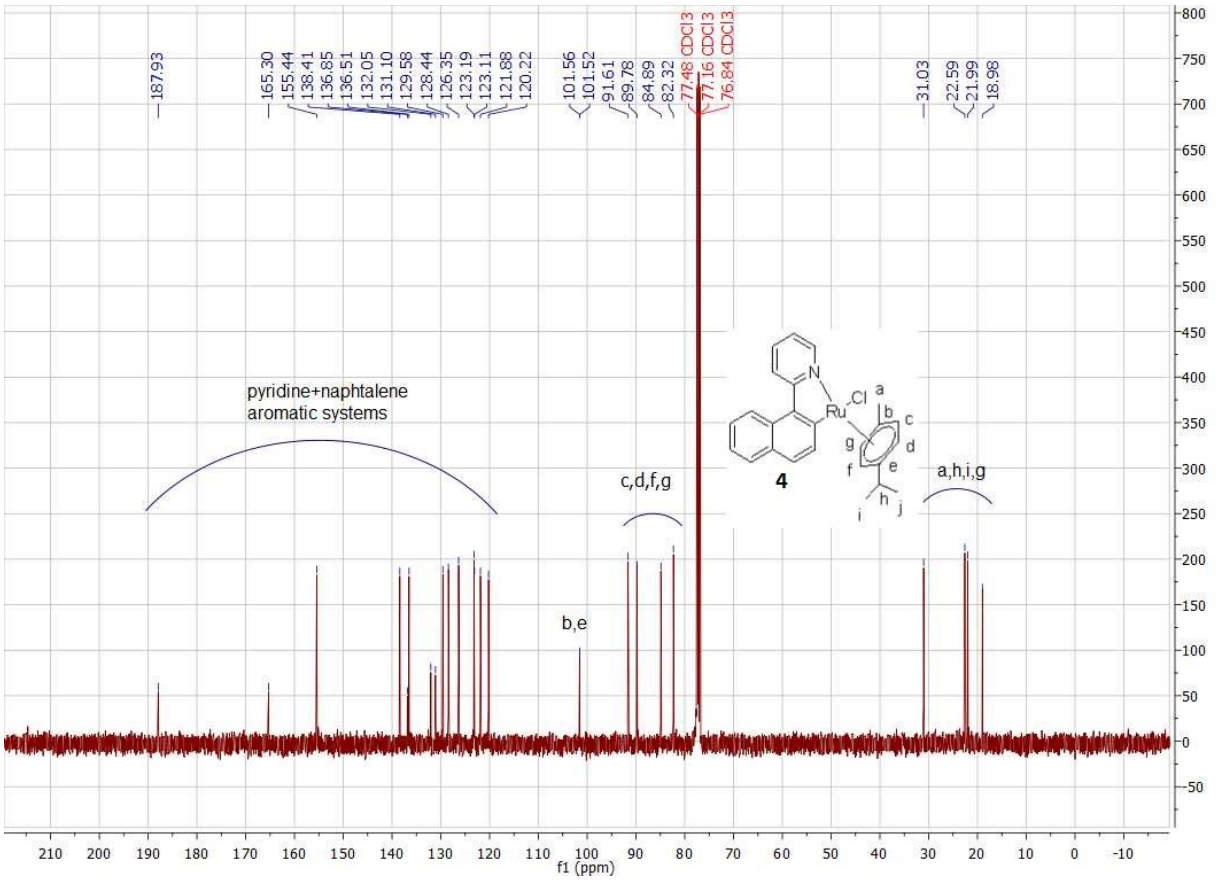

Figure S5. $^{13}C\{^{1}H\}$ NMR spectrum (400 MHz, $CDCl_3$) of compound **4**

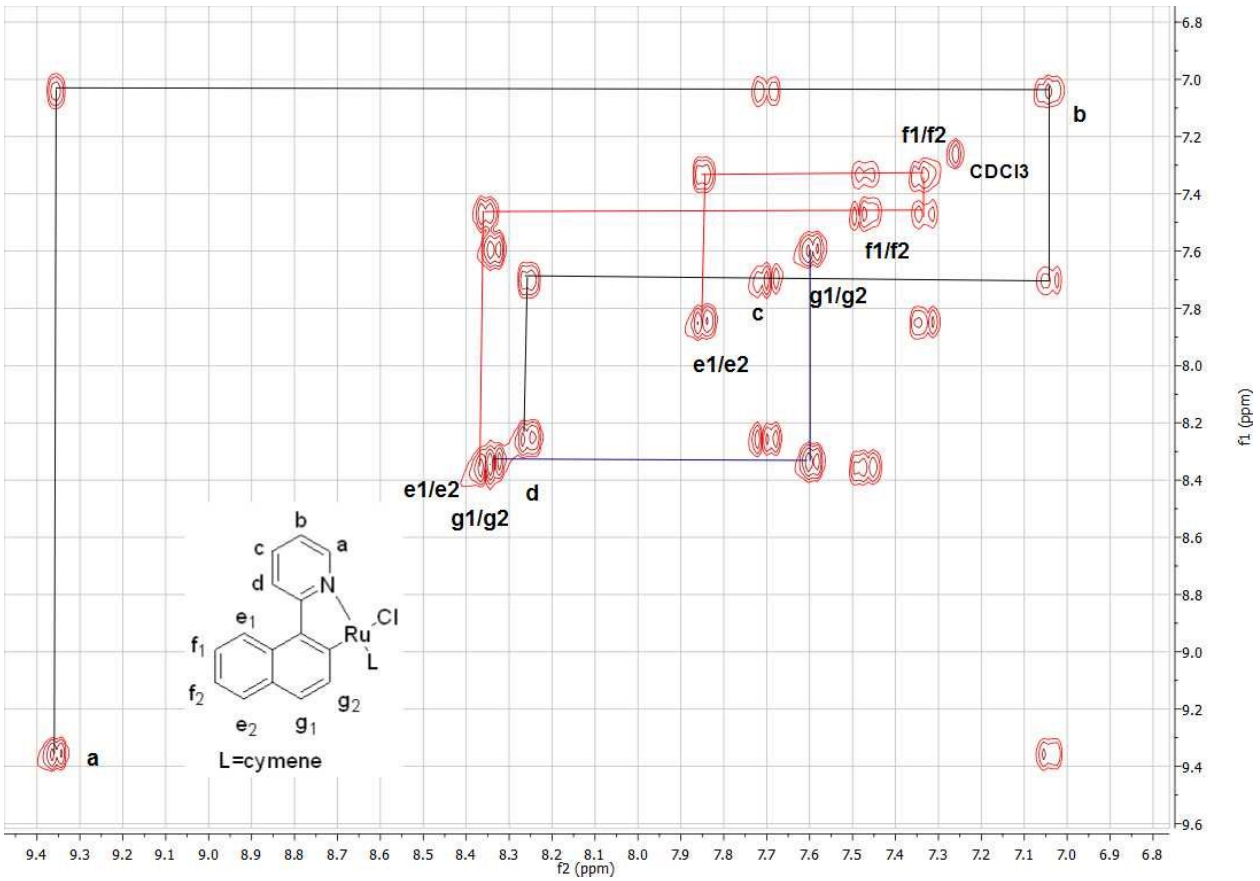

Figure S6. Low-field aromatic region of the COSY NMR spectrum (400 MHz, $CDCl_3$) of compound **4**

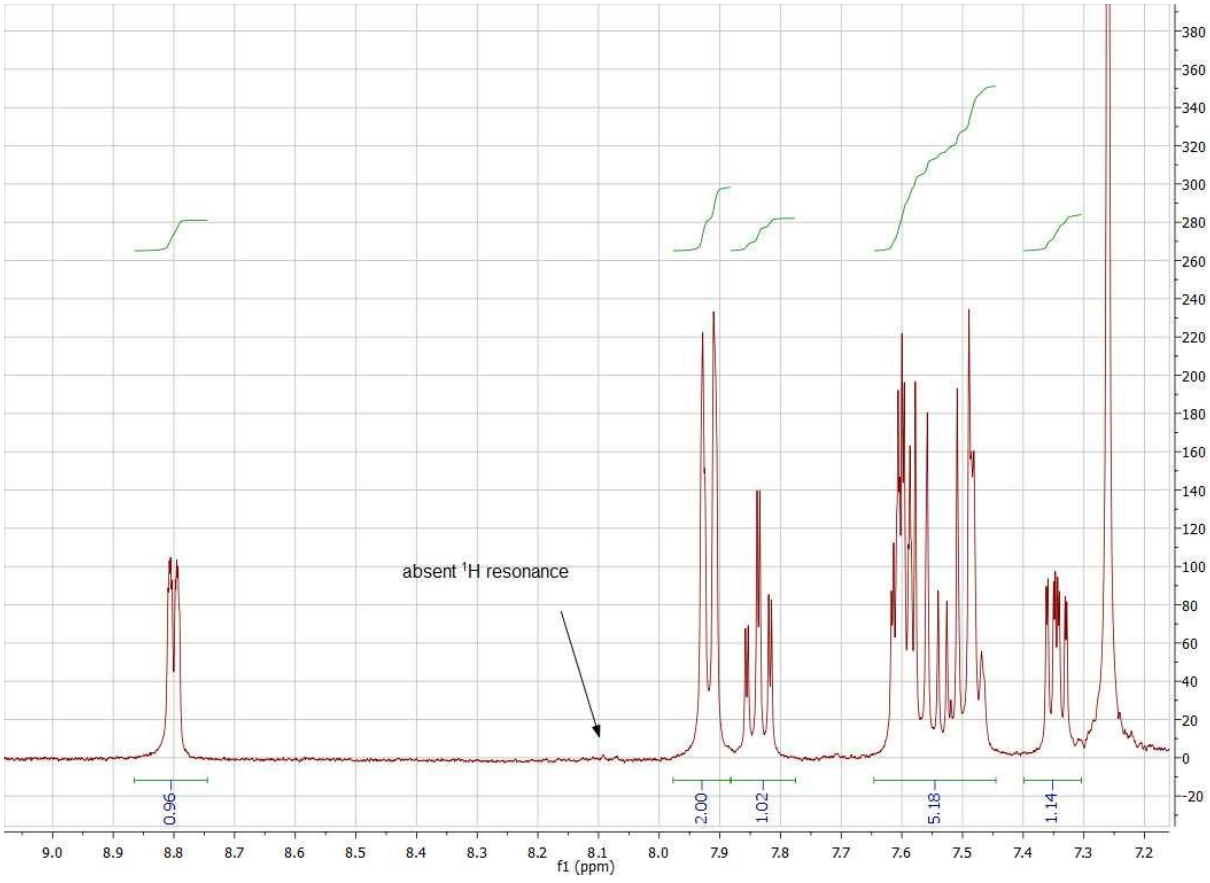

Figure S7. ^{1}H NMR spectrum (400 MHz, $CDCl_3$) of δ-deuterated compound **1-*da***

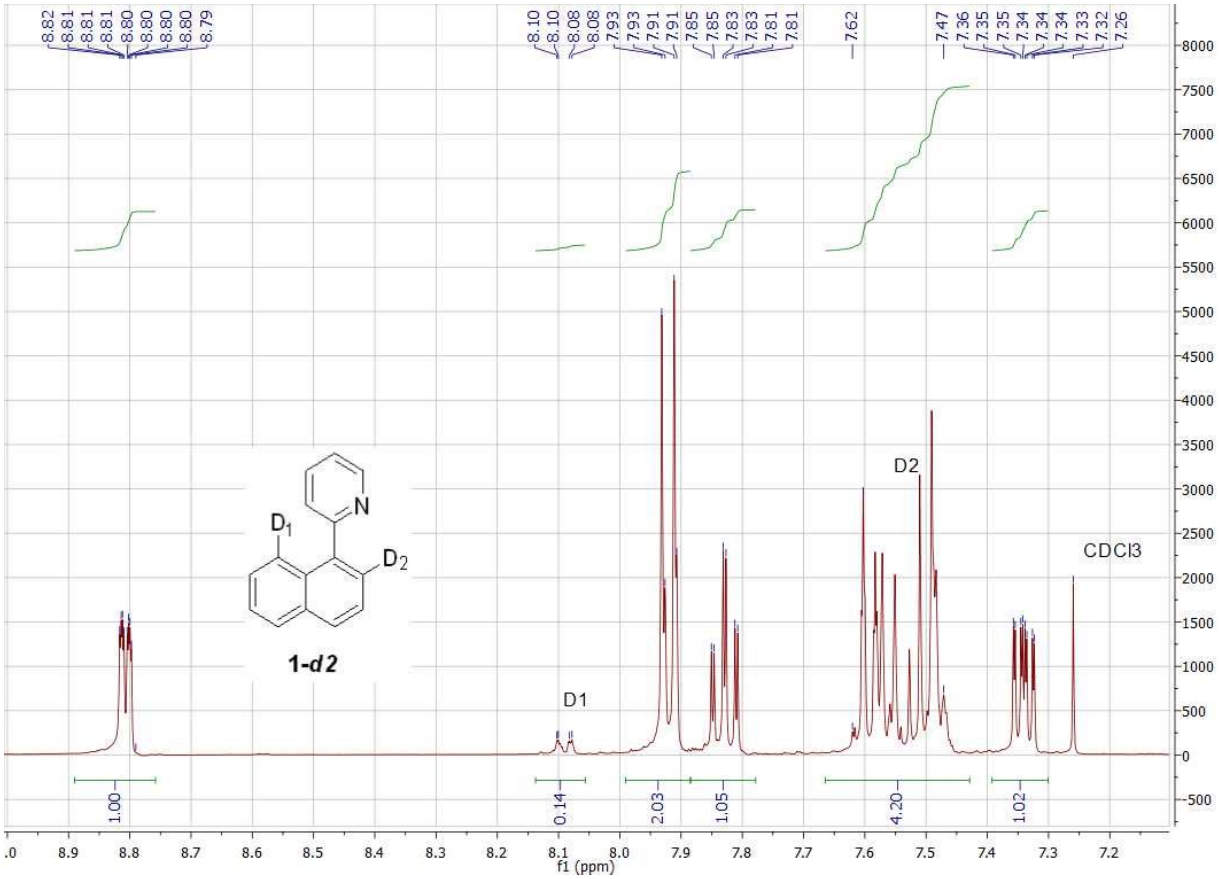

Figure S8. ^{1}H NMR spectrum (400 MHz, $CDCl_3$) of bis-deuterated compound **1-*d2***

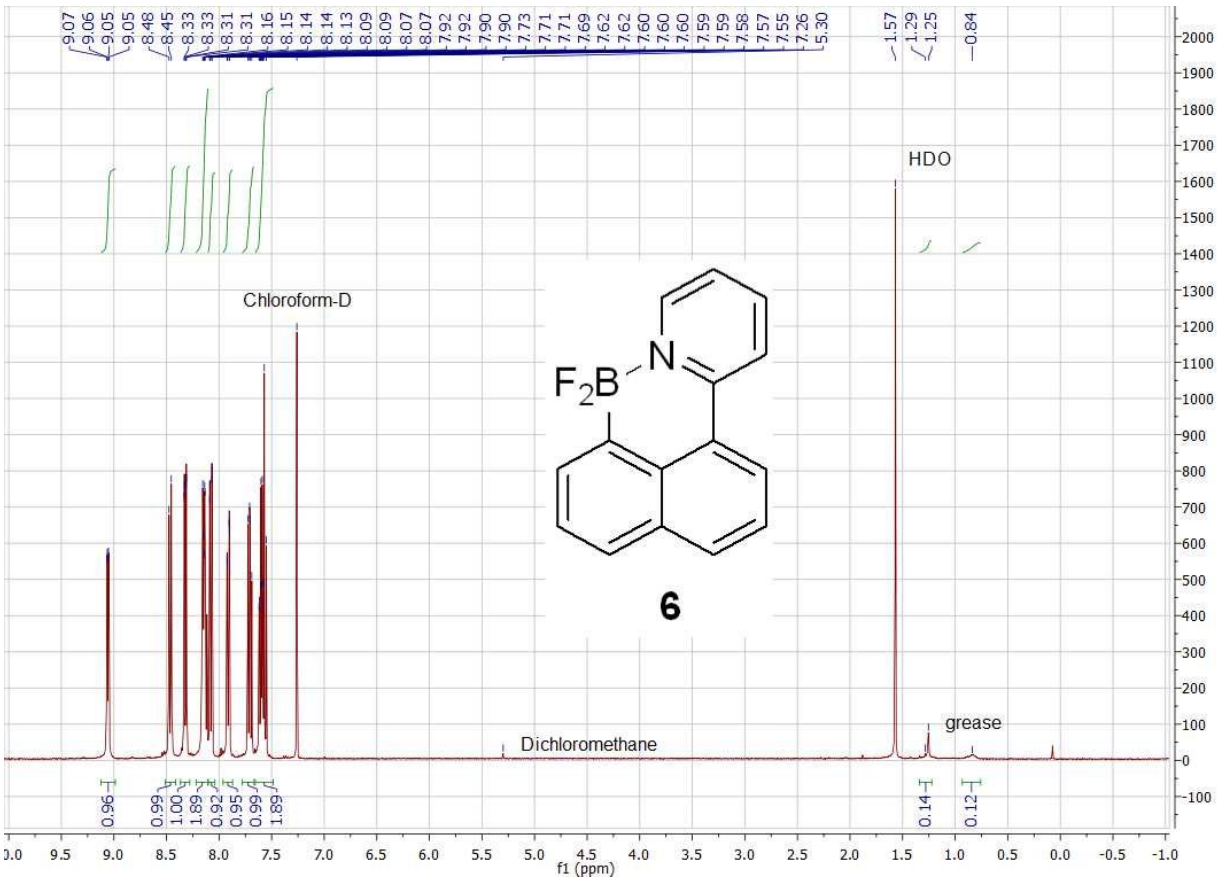

Figure S9. ^{1}H NMR spectrum (400 MHz, $CDCl_3$) of compound **6**

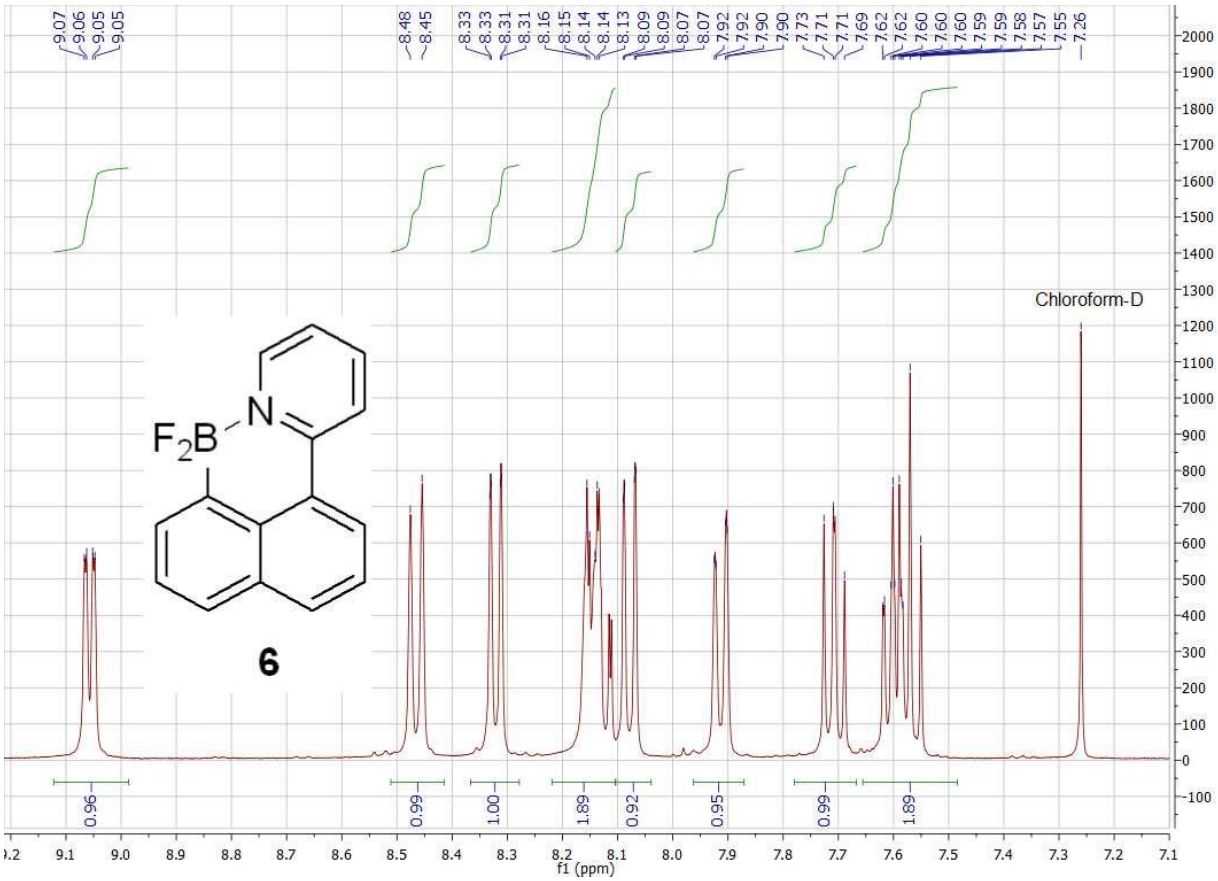

Figure S10. Aromatic region of the ^{1}H NMR spectrum (400 MHz, $CDCl_3$) of compound **6**

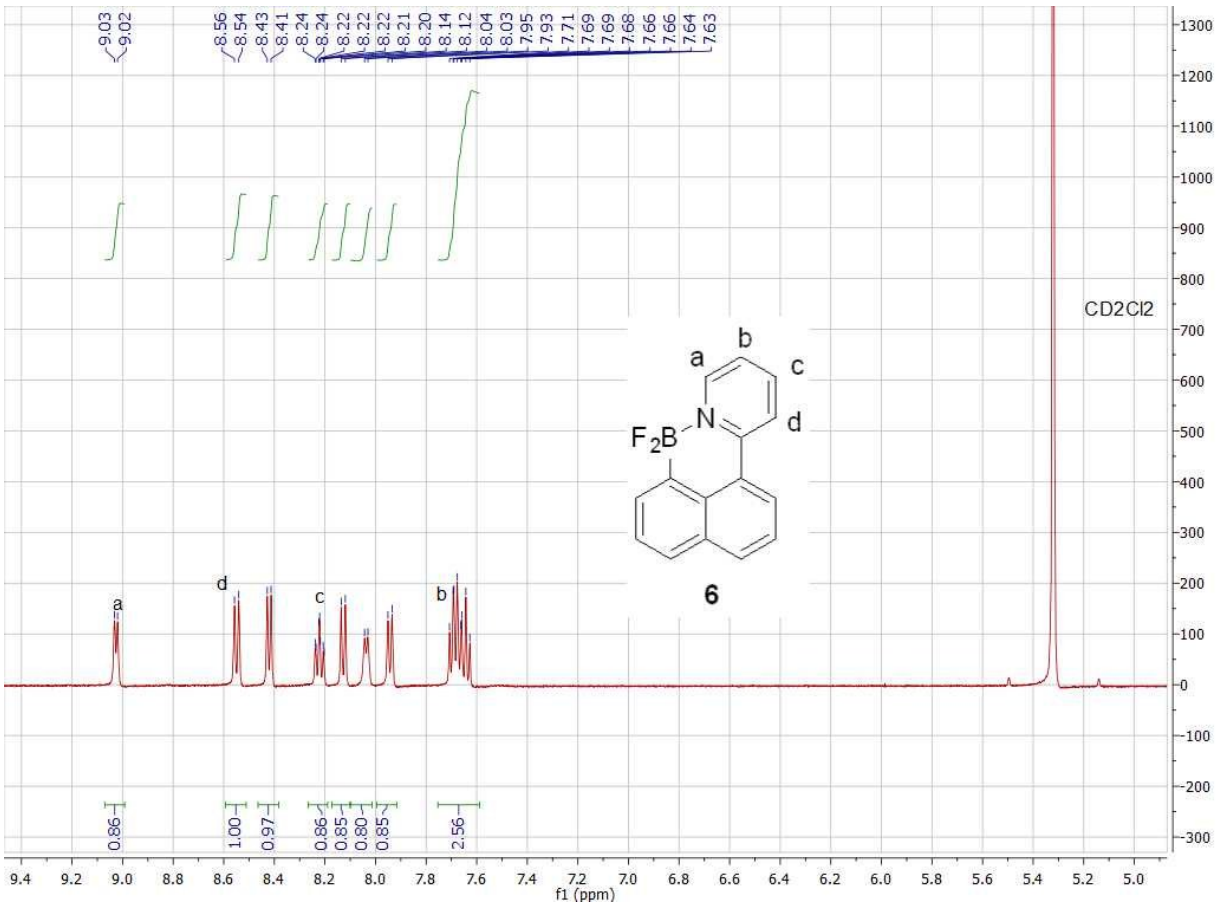

Figure S11. Aromatic region of the ^{1}H NMR spectrum (500 MHz, CD_2Cl_2) of bis-deuterated compound **6,** which was found to have better resolution of the resonances, than a spectrum in $CDCl_3$ and was used for gCOSY analysis.

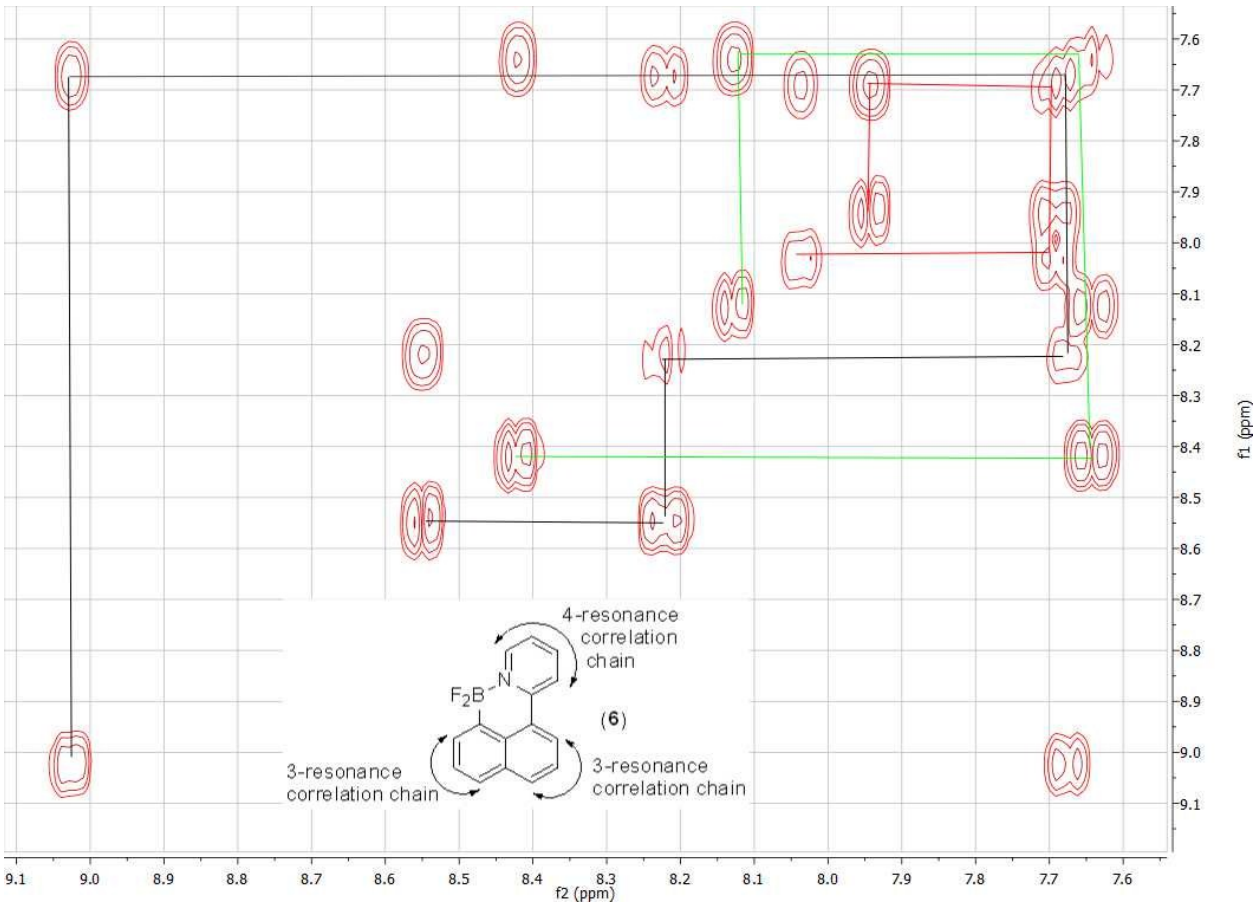

Figure S12. Aromatic region of the COSY NMR spectrum (500 MHz, CD_2Cl_2) of compound **6**

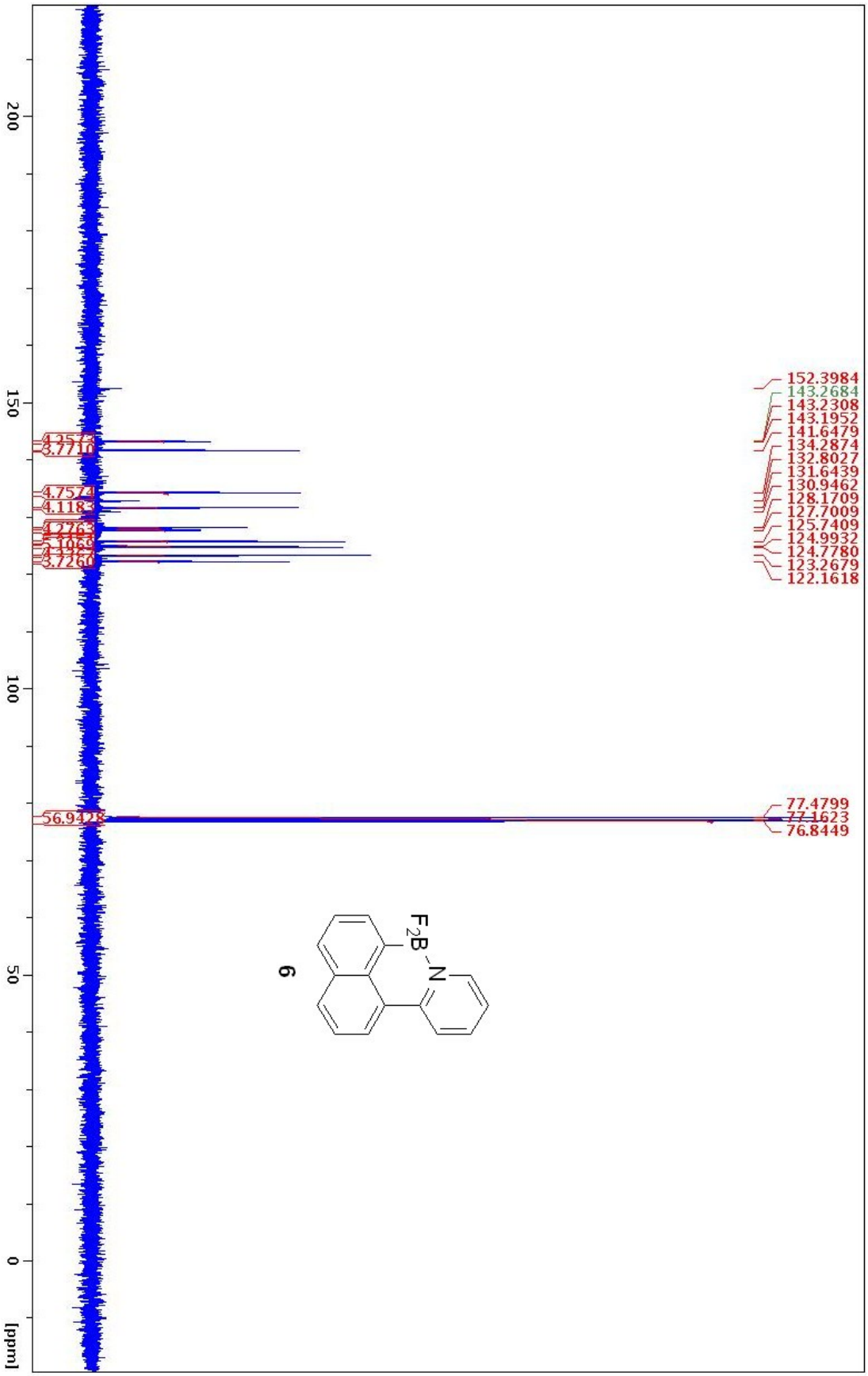

Figure S13. $^{13}C\{^{1}H\}$ NMR spectrum (400 MHz, $CDCl_3$) of compound **6**